Wave-Coupled $LiNbO_3$ Electrooptic Modulator for Microwave and Millimeter-Wave Modulation

William B. Bridges, Finbar T. Sheehy, and James H. Schaffner

***Abstract*—The phase velocity mismatch due to material dispersion in traveling-wave $LiNbO_3$ optical waveguide modulators may be greatly reduced by breaking the modulation transmission line into short segments and connecting each segment to its own surface dipole antenna. The array of antennas is then illuminated by the modulation signal from below at the proper angle to produce a delay from antenna to antenna that matches the optical waveguide's delay. A phase modulator 25 mm in length with five antennas and five transmission line segments was operated from 4.6 to 13 GHz with a maximum phase modulation sensitivity over $100°/W^{1/2}$.**

Introduction

TRAVELING-WAVE optical waveguide modulators in $LiNbO_3$ have shown frequency responses greater than 20 GHz. Unfortunately, both high frequency response and high sensitivity are difficult to realize in the same device. The mismatch in phase velocities between the optical wave and the microwave signal due to material dispersion in $LiNbO_3$ limits the interaction length and hence the sensitivity. This paper describes a new technique to overcome the material dispersion limitation, and as an added benefit, utilizes a waveguide medium to introduce the modulation signal. This latter feature may prove as important as the former in extending modulator operation to the millimeter wave range.

Alferness *et al.* [1] overcame the dispersion limitation by dividing the modulation electrodes into sections whose length produces a 180° differential phase error from end to end at the center of a passband. The ends of one section are then connected to the next by transposed leads to correct the phase by 180°. In this way the average phase velocity of the modulating wave follows the optical phase velocity. Unfortunately, the length of each section results in a loss in sensitivity.

Schaffner [2] recently described a technique that also divides the electrodes into sections, but each section is shorter than the length that produces 180° phase error. The next section is connected to the previous section through a stub transmission line that provides a phase delay equal to 360° minus the phase error suffered in the short modulator section. As in [1], the average modulating wave velocity is equal to the optical velocity, but the freedom to choose shorter sections means that less penalty per section is suffered.

Manuscript received August 30, 1990; revised November 21, 1990. Preliminary results of this paper were presented in paper OE 7.2 at the LEOS Annual Meeting, Boston, MA, November 7, 1990. This work was supported by a grant from the Caltech President's Fund and a grant from Rome Air Development Center.

W. B. Bridges and F. T. Sheehy are with the Division of Engineering and Applied Science, California Institute of Technology, Pasadena, CA 91125.

J. H. Schaffner is with Hughes Research Laboratories, Malibu, CA 90265.

IEEE Log Number 9042486.

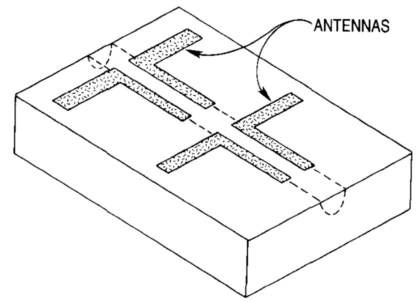

Fig. 1. Schematic drawing of two dipole antennas and connected transmission line sections on the surface of a waveguide E-O modulator.

We report still another technique to realize phase matching on the average. As in [2], the modulator electrodes are divided into short sections, but each section is connected to its own surface antenna as shown in Fig. 1. This array of antennas is then illuminated from the substrate side by a plane wave at an angle Θ with respect to the surface normal, the angle chosen so that the phase velocity of the incident modulating wave in the direction of the optical waveguide is equal to that of the optical wave. That is, $\Theta = \sin^{-1}(n_o/n_m)$ where n_o is the optical refractive index and n_m is the modulation refractive index. (A similar angle phase matching was demonstrated by Kaminow *et al.* [3] for a *bulk* $LiNbO_3$ electrooptic modulator.) Thus, each antenna receives the proper phase to match the phase velocity of the optical wave. As the wave from the antenna travels down the short transmission line section, a phase error develops, but this is kept small by making the section short.

Since no physical connections are made to the antennas, no parasitic circuit elements are introduced that limit scaling to higher frequencies. Likewise, the effect of loss in the transmission line segments is minimized since the array of line segments is fed from the side and not the end. In return for these advantages, we must develop an efficient method of coupling energy into the antennas from a waveguide feed.

Experimental Phase Modulator

Fig. 2 shows a photolithographic mask for five modulator electrode segments with attached antennas designed for a 12 GHz center frequency. The overall modulator length is 25 mm. A simple phase modulator was built rather than a Mach-Zehnder amplitude modulator; however, the same mask should also work if applied to one arm of a M-Z. The antennas were configured as "two half waves in phase," and the modulator electrodes were also a half wave long at 12 GHz. In designing both the antennas and the transmission lines an effective refractive index of 3.8 was taken as the proper average of $LiNbO_3$ and air for

1041-1135/91/0020-0133$01.00 ©1991 IEEE

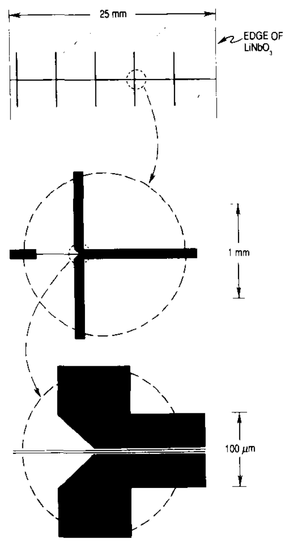

Fig. 2. Photolithographic mask for five antennas-plus-transmission lines covering a 25 mm long optical waveguide. Magnified details are shown in the lower two drawings.

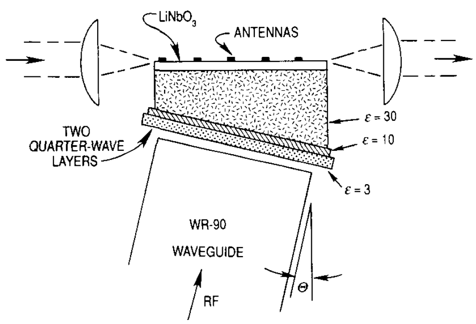

Fig. 3. Schematic side view of an experimental modulator showing $LiNbO_3$ wafer with antennas, input and output lenses, a wedged block of high dielectric constant material, quarter-wave matching layers, and microwave waveguide. The waveguide feed was changed to WR-137 for 4.6-7 GHz measurements.

electrodes on the dielectric surface. The optical waveguide was formed by titanium diffusion, and was about 6 μm in size.

As shown in Fig. 3, the $LiNbO_3$ plate was attached to a wedge of dielectric with $\epsilon = 30$. A wedge was used to introduce the modulating wave into the block at the calculated optimum angle of 23° since the critical angle for $LiNbO_3$ is about 9°. Two matching layers of intermediate dielectric constant were introduced to minimize the reflection at the interface. The beam from a single-frequency He-Ne laser at 633 nm was coupled in and out with microscope objectives. The optical power was kept low to minimize optical damage.

The pattern of a dipole antenna on the surface of a dielectric is strongly directed into the dielectric; for $\epsilon = 30$, there is virtually no coupling to the air side. The pattern has a strong lobe in the direction of the critical angle (9° here). We have used the theory given by Engheta *et al.* [4] to estimate the pattern at the desired angle of 23°, and find that it is only about 0.5 dB down from the peak.

We used a scanning Fabry-Perot interferometer to detect the phase modulated signal. Fig. 4 shows the display for modulation

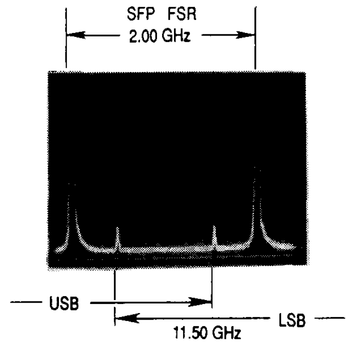

Fig. 4. Oscilloscope display of scanning Fabry-Perot (SFP) output with 11.50 GHz narrow deviation phase modulation. The He-Ne laser output was single frequency (large pips at the free spectral range (FSR) spacing). The phase modulation sidebands are the smaller pips. The apparent spacing of 1.5 GHz is due to the aliasing by the SFP.

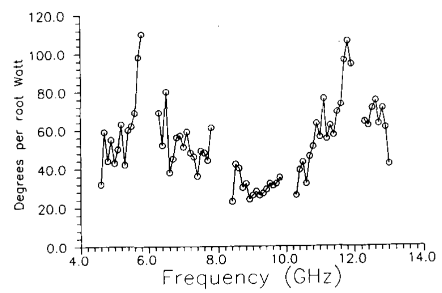

Fig. 5. Modulator sensitivity in degrees of phase modulation per watt$^{1/2}$ of microwave drive power as a function of drive frequency.

at 11.50 GHz. Since the free spectral range of 2 GHz is much less than the modulation frequency, there is an aliasing every 2 GHz, and the sidebands appear to be at $11.50 - 5 \times 2.0 = 1.5$ GHz. The modulator phase deviation can be deduced from the amplitude of the sidebands relative to the carrier for narrow deviation phase modulation from the formula [5]

$$\Delta\phi = 2[P_{\text{sideband}}/P_{\text{carrier}}]^{1/2}. \tag{1}$$

This measurement technique has the advantage of not requiring a fast photodetector and is thus equally effective for 4.6-13 GHz modulation, 60 GHz modulation, or any other frequency.

Fig. 5 shows the phase deviation normalized to the square root of the microwave drive power as a function of modulation frequency. The gaps at 6, 8, 10, and 12 GHz are regions where measurements were difficult since the sidebands fall on top of the aliased carriers in the SFP display. The structure on this curve has several possible sources: antenna and electrode resonance, reflections within the wedge, and at the $LiNbO_3$-air interface, . . . However, we obtain a reasonable fit with a simple model of the antenna and open-circuited transmission line impedances, and modulation resulting from forward and reflected waves on the line [6]. There are two resonance peaks in the response: one around 6 GHz where the antenna elements and transmission line segments are each a quarter wave in length, and another around 12 GHz (the design value) where they are a half wave in length. The absolute value of $100°/W^{1/2}$ is not too much less than conventional microwave modulators [7].

A number of different feed wedges was used to establish the effect of illumination angle on performance. Fig. 6 shows the

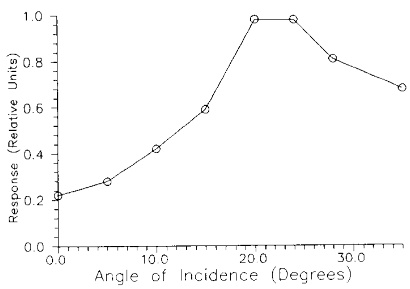

Fig. 6. Average modulator response as a function of angle of incidence of modulating signal.

average response over the 9–12 GHz range at each illumination angle. The response peaks at about 23° as expected, confirming the phase-velocity-matching picture.

Summary

We have demonstrated a new technique of phase velocity matching in electrooptic modulators by illuminating an array of antennas each connected to its own short section of modulating electrode. Promising sensitivity results of $100°/W^{1/2}$ were obtained at 12 GHz.

Note Added in Proof: We have recently obtained approximately $80°/W^{1/2}$ phase modulation at 61 GHz with an 18 mm array of 20 antenna/transmission-line segments of one-sixth the dimensions indicated in Fig. 2.

Acknowledgment

The authors wish to acknowledge the technical support of R. L. Joyce and R. E. Johnson, and many valuable discussions with R. W. Terhune.

References

[1] R. C. Alferness, S. K. Korotky, and E. A. J. Marcatili, "Velocity-matching techniques for integrated optic traveling wave switch modulators," *IEEE J. Quantum. Electron.*, vol. QE-20, pp. 301–309. Mar. 1984.

[2] J. H. Schaffner, "Analysis of a millimeter wave integrated electro-optic modulator with a periodic electrode," in *Proc. SPIE OE-LASE Conf. 1217*, paper 13, Los Angeles, CA, Jan. 16–17, 1990, pp. 101–110.

[3] I. P. Kaminow, T. J. Bridges, and M. A. Pollack, "A 964-GHz traveling-wave electro-optic light modulator," *Appl. Phys. Lett.*, vol. 16, pp. 416–418, June 1, 1970.

[4] N. Engheta, C. H. Papas, and C. Elachi, "Radiation patterns of interfacial dipole antennas," *Radio Sci.*, vol. 17, pp. 1557–1566, Nov.–Dec. 1982.

[5] See, for example, *Reference Data for Radio Engineers*. 5th Ed. New York: Howard Sams, 1968, Section 21-7.

[6] F. T. Sheehy, unpublished calculations.

[7] D. Erasme, D. A. Humphreys, A. G. Roddie, and M. G. F. Wilson, "Design and performance of phase reversal traveling wave modulators," *J. Lightwave Technol.*, vol. 6, pp. 933–936, June 1988.